Seismic anisotropy in the mantle transition zone beneath Fiji-Tonga

Wang-Ping Chen and Michael R. Brudzinski[1]
University of Illinois, Urbana, Illinois, USA

Received 24 September 2002; revised 24 February 2003; accepted 10 March 2003; published 5 July 2003.

[1] We demonstrate a rare, unequivocal case of anisotropy in the transition zone (TZ), evident from many horizontal-polarized shear-waves (*SH*) that arrive up to 3 s earlier than vertical-polarized shear-waves (*SV*). The anisotropic region correlates with deep earthquakes away from the active subduction zone and known boundaries of lateral heterogeneities in compression- and shear-wave speeds. We interpret the anisotropy as strong fabric associated with a large petrologic anomaly in the core of remnant lithosphere which is buoyant and stagnates in the TZ. Fast subduction of cold slab actually favors such a configuration, so slab penetration into the lower mantle does not uniformly occur. *INDEX TERMS:* 7203 Seismology: Body wave propagation; 3699 Mineralogy, Petrology, and Mineral Physics: General or miscellaneous; 7207 Seismology: Core and mantle; 8120 Tectonophysics: Dynamics of lithosphere and mantle—general; 8124 Tectonophysics: Earth's interior—composition and state (1212). **Citation:** Chen, W.-P., and M. R. Brudzinski, Seismic anisotropy in the mantle transition zone beneath Fiji-Tonga, *Geophys. Res. Lett.*, *30*(13), 1682, doi:10.1029/2002GL016330, 2003.

1. Introduction

[2] Seismic anisotropy is critical for understanding mantle dynamics because it is one of few means to delineate mantle flow. Near important boundary layers, concentrated horizontal flow is expected to create strong seismic anisotropy [e.g., *Karato*, 1998]. However, at depths greater than about 200 km, evidence for seismic anisotropy is sparse [e.g., *Savage*, 1999; *Silver*, 1996]. Previous work often involves observations at long periods and therefore has limited spatial resolution [e.g., *Trampert and van Heijst*, 2002]. Furthermore, the amount of anisotropy appears to be small in the transition zone of the mantle (TZ) and near the 660-km discontinuity [e.g., *Savage*, 1999]—key areas for understanding thermal convection and chemical mixing in the mantle [e.g., *Lay*, 1994; *Silver et al.*, 1988].

[3] Along the Tonga subduction zone, where a vast amount of old, cold lithosphere is subducting at a staggering rate of over 200 mm/yr [*Bevis et al.*, 1995], *Wookey et al.* [2002] reported variations in shear-wave speeds (V_S) consistent with polarization anisotropy (birefringence) just below the TZ. Unfortunately, the seismic data are too complex to model, hindering tectonic interpretations. Here we demonstrate a rare, unequivocal case of strong anisotropy in the TZ beneath the Fiji-Tonga region using a uniform set of high-resolution broadband waveforms. The dataset includes clear arrivals of *SH* that lead *SV* with a split time (δt) of up to 3 s (Figure 1), indicating V_{SH} is higher than V_{SV} by ~1% in the TZ. By synthesizing anisotropy, heterogeneities in *P*- and *S*-wave speeds, fault plane solutions, seismicity, and data from experimental rock physics, we report new findings about how an anisotropic, petrologic anomaly develops and evolves when a large slab of cold lithosphere enters the TZ.

2. Data Analysis and Results

[4] We use digital seismograms from stations NOUC and PVC in the back-arc, and RAR in the fore-arc (Figure 1a). Overall, 204 waveforms of high signal-to-noise ratios are modeled by synthetic seismograms (Table S1)[2]. The key observation is that for paths in Region I, *SH* always leads *SV* with large δt of up to 3 s (Figure 1).

[5] The average δt in Region I is 1.4 ± 0.5 s (one standard deviation, SD). Such an SD is comparable to uncertainties in measuring δt, or 1/6 of the dominant period of individual pulses (Figure 2a). Large birefringence disappears suddenly in the rest of the back-arc, Regions II–III, where δt scatters around zero (±0.4 s) with no obvious pattern and without any $\delta t > 1$ s (Figures 1 and 2b). Values of 0 ± 0.4 s are indistinguishable from nine observations beneath the fore-arc prior to subduction (δt 0 ± 0.3 s; Table S1) or background level of the average Earth [e.g., *Savage*, 1999], all showing null birefringence. The abrupt change from strong birefringence in Region I to null birefringence farther south coincides with the southern termination of outboard earthquakes (OE)—a zone of deep seismicity extending ~1000 km away from the Wadati-Benioff zone (WBZ) (Figure 1).

[6] Birefringence in Region I is most likely a result of anisotropy in the TZ. First, the amount of birefringence relates to the turning depth of rays. All δt greater than 1 s are from rays turning in the TZ (grey squares, Figure 1b). Conversely, rays turning below the TZ have the smallest δt (solid squares). Second, within a small azimuthal range, observed birefringence inversely relates to focal depths, reflecting decreasing length of ray-paths within the TZ. For instance, overall appearance of waveforms is similar between events I2 and I3 (Figure 2a), except that the shallower event (I2, ~590 km) exhibits a δt of 2 s, nearly

[1] Now at Department of Geology and Geophysics, University of Wisconsin at Madison, USA.

[2] Supporting material (Table S1) is available via Web browser or via Anonymous FTP from ftp://ftp.agu.org, directory "apend" (Username = "anonymous," Password = "guest"); subdirectories in the ftp site are arranged by paper number. Information on searching and submitting electronic supplements is found at http://www.agu.org/pubs/esupp_about.html.

0094-8276/03/2002GL016330$05.00

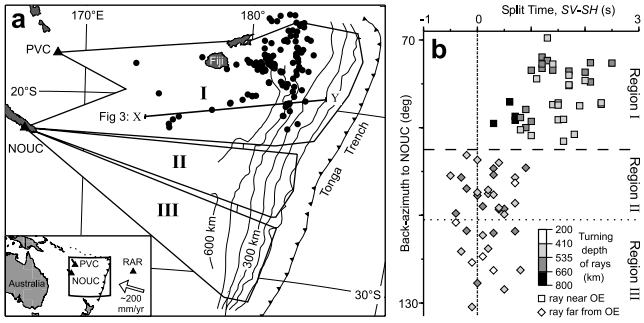

Figure 1. (a) Map showing experimental configuration. Based on high-resolution waveforms recorded at permanent seismographs (triangles), clear lateral variations in seismic anisotropy and seismic wave speeds delineate three distinct regions in the TZ (I–III) [*BC2000*; *BC2003*]. Contours show position of the WBZ and solid circles are OE [*CB2001*]. (b) Plot of split time between *SV* and *SH* (δt) as a function of back azimuth. Only δt of first arrivals are plotted as they can be easily verified by visual inspection. Prominent anisotropy occurs throughout Region I, where OE occur. In contrast, Regions II and III show null birefringence.

twice as large as that of the deeper event near the bottom of the TZ (I3, ~660 km). Since the Fresnel zone (radius ~60 km in TZ) of rays from the two distinct events overlap near the common seismograph but are far apart in the TZ, the observed difference in δt must arise in the TZ (Figure 3a).

[7] Third, for triplicate waveforms, δt for each arrival is commensurate with the length of ray-path in the TZ. For event I1, the first arrival C′A grazes the upper portion of the TZ (Figures 2d and 2e) and shows a δt of 1.5 s (Figure 2a). In contrast, arrivals BC and CD (cusp C) dive deep into the TZ and the δt increases accordingly to a remarkable value of 2.7 s (Figures 2a and 2e). Since rays comprising a triplicate waveform have paths that spread far apart in the TZ but converge near the station (Figure 2e), only anisotropy in the TZ can cause different δt among arrivals. This reasoning also rules out anisotropy near the source as a primary factor for the observed δt, since triplicate arrivals that exhibit different δt have comparable ray-paths near the source.

[8] Modeling of waveforms and δt by synthetic seismograms indicate that the amount of anisotropy in the TZ is about 0.9 ± 0.3% (Figure 2c). Here we assume radial anisotropy with the vertical axis as the slow direction of polarization (*SV*)—simplest case considering the limited azimuthal coverage and the subhorizontal geometry of most ray-paths (Figures 1a and 3a). We calculate synthetic seismograms using ANRAY and reflectivity [*Fuchs and Mueller*, 1971; *Gajewski and Psencik*, 1987]. In the latter, radial anisotropy is simulated by fine (~1 km in thickness), isotropic layers of alternating high and low V_S (10% contrast for 1% anisotropy) [e.g., *Backus*, 1962]. The two approaches result in essentially identical results whenever the ray-theoretical approach of ANRAY is valid.

[9] Synthetic seismograms from this simple model match observed broadband waveforms well, including differences in δt among different arrivals of triplicate waveforms (Figure 2a). Furthermore, the model accounts for observed δt throughout Region I. The mean misfit in δt of all first arrivals is less than 0.1 ± 0.4 s, comparable to the scatter of null birefringence in Regions II–III or uncertainties in measuring δt (Figure 1b).

[10] We also test variations of the simplest model and the amount of anisotropy must either stay constant or decrease with depth in the TZ. For instance, a linear gradient in anisotropy, from 1.2% to 0.3% at the top and bottom of the TZ, respectively, works as well as the simplest model. Likewise, a stepwise decrease in anisotropy from 1.0% to 0.5% near a depth of 535 km is equally plausible.

[11] In addition to the correspondence in map view (Figure 1a), there is vertical correlation between anisotropy and OE. Figure 3a illustrates the dense coverage of rays near hypocenters of OE. δt of 1–3 s are observed along each

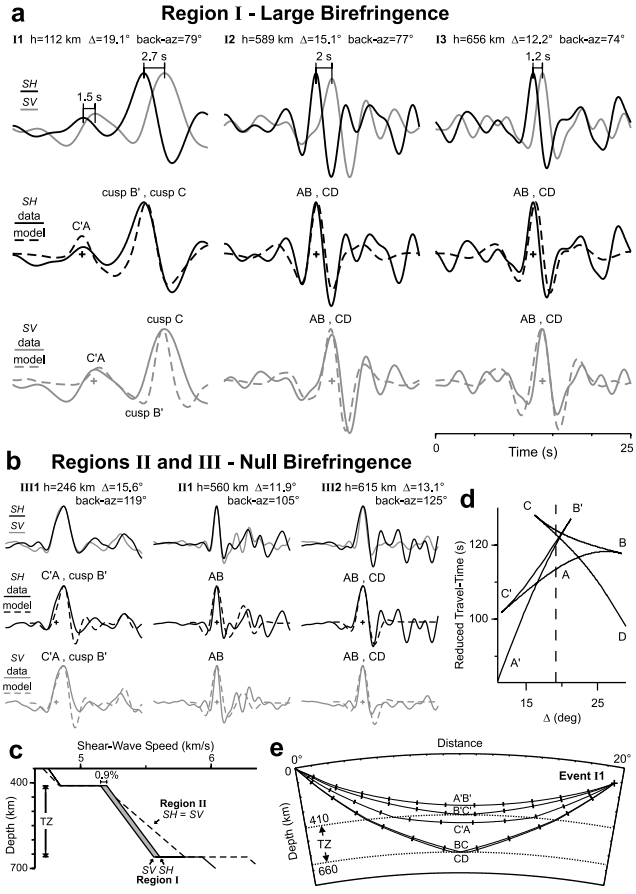

Figure 2. Comparison between observed (solid traces) and synthetic (dashed traces) broadband seismograms at NOUC. We plot deconvolved, bandpass-filtered (~0.1 to ~0.5 Hz) seismograms in which an arrival from the forward branch of a triplication corresponds to the peak of an acausal, symmetric wavelet. (a) Results from the simplest anisotropic model (Figure 2c) for Region I. Notice that distinct δt of different pulses are matched well. (b) Results from the isotropic model for Regions II and III. (c) V_s as a function of depth. In Region I, V_{SV} is ~1% less than V_{SH} in the TZ. In Region II, V_{SH} equals V_{SV}, both being ~3% greater than those in Region I. (d) Travel-times (reduced by 10 km/s) for event I1 at the vertical line). (e) A cross-section showing ray-paths (solid curves) for event I1. Short bars mark intervals of 40 s.

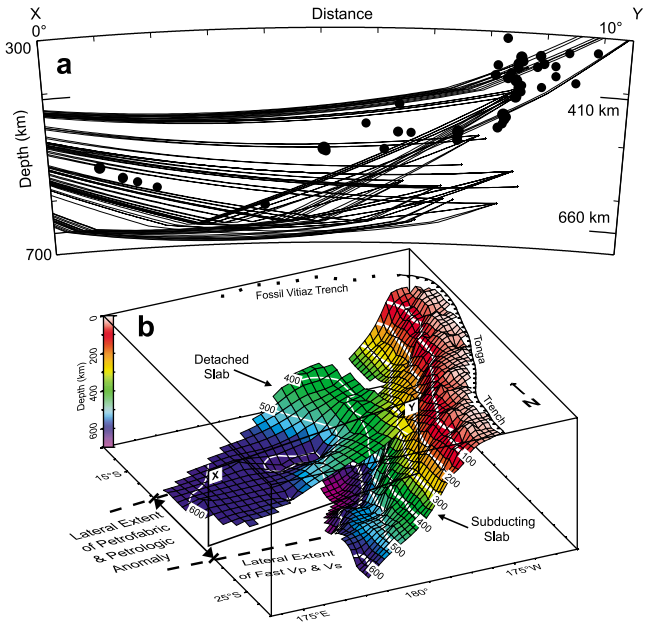

Figure 3. (a) Representative cross-section of anisotropic Region I. Solid curves are *SH* and *SV* ray-paths (from ANRAY) for waveforms analyzed in this study. Notice the dense coverage of paths throughout the TZ, including the source zone of OE (solid circles). Width of cross-section is 400 km. (b) 3-D rendition of seismicity near Tonga. Two separate surfaces, representing a detached remnant of slab and the actively subducting lithosphere, are constructed from hypocenters of OE and those in the WBZ, respectively [*CB2001*]. A strong petrofabric apparently accompanies a petrologic anomaly in the core of detached, buoyant slab.

path turning in the TZ (Figure 1b). Thus the source zone of OE must be highly anisotropic. In contrast, null birefringence beneath the fore-arc, a region not affected by subduction, indicates that strong anisotropy in the back-arc must be caused by subduction. Since observations of anisotropy in the TZ are rare in general [e.g., *Savage*, 1999], remarkable birefringence beneath Region I suggests that a critical tectonic process, not easily detectable along other subduction zones, stands out near Tonga.

3. Interpretations and Discussion

[12] To form seismic anisotropy, lattice-preferred orientation (LPO) of anisotropic minerals or shape-preferred orientation (SPO) of secondary phases must be abundant and aligned into a strong petrofabric. An in-depth understanding of how this petrographic anomaly arises beneath the back-arc comes from a synthesis of complementary constraints. It is a basic tenet of plate tectonics that deep earthquakes occur in the cold interior of subducted slab [*Isacks and Molnar*, 1971]. Otherwise, deep earthquakes would not be restricted to zones of recent convergence. It follows that OE are sufficient evidence for low temperature where seismic anisotropy stands out (Figure 1b).

[13] In the TZ, V mainly reflect variations in petrology and temperature. Low temperature raises seismic wave speeds so one would expect the cold, anisotropic region associated with OE to have high V. Surprisingly, corresponding patterns of high V_P and V_{SH} occur only in a restricted region immediately to the south of OE (Region II, Figure 1a) [*Brudzinski and Chen*, 2000; 2003 (*BC2000*; *BC2003*)]. The seismogenic zone (Region I) has moderate values of V_P and V_{SH} similar to those beneath Region III and the fore-arc—a region not affected by subduction. The drop in V_P and V_{SH} from Region II to Region I is ~3% and occurs over a distance <30 km [*BC2003*]. It is perhaps not surprising that such abrupt features, established by detailed modeling of hundreds of high-resolution broadband waveforms, were not resolved by travel-time tomography with >200 km cell sizes.

[14] We emphasize that both anisotropy and lateral heterogeneity occur in the TZ beneath the back-arc of Tonga. First, polarization anisotropy does not apply to *P*-waves so observations shown in Figure 1a do not affect the demarcation of lateral heterogeneity that can be established from V_P alone [*BC2000*]. Second, anisotropy only exists in Region I where V_{SV} is always less than V_{SH}, so the reduction in V_{SV} as one crosses from Region II to Region I would be about 4%, even larger than the 3% difference in V_{SH}.

[15] Considering the strong evidence against high V_P and V_{SH} where OE occur, the effect of low temperature to raise V in the source region of OE must be counteracted by a petrologic anomaly, such as compositional or mineralogical variations. The sharp boundary between Regions I and II, where OE cease and V_P and V_{SH} abruptly rise (Figure 1), is also consistent with petrologic variations, since temperature variations alone would produce a gradual change [*BC2003*]. Such a petrologic anomaly must also have a pervasive petrofabric to account for its strong anisotropy.

[16] Contenders for the petrologic anomaly must have the potential to trigger deep earthquakes and lower V_P and V_S. Possible candidates include metastable phases such as olivine (α-phase), volatiles in the form of hydrous phases, or partial melt induced by volatiles [e.g., *Faul et al.*, 1994; *Green and Burnley*, 1989; *Kirby et al.*, 1991; *Meade and Jeanloz*, 1991]. Those materials must be brought down to the TZ by subduction, and the anisotropic zone of OE is a region where impounding of subducted material is most significant, favoring accumulation of metastable olivine or volatiles [*BC2000*]. This condition is most easily met in Tonga where old lithosphere is subducting at a staggering rate. Combining this reasoning with 1000 focal mechanisms and 6600 relocated hypocenters, *Chen and Brudzinski* [2001] (*CB2001*) identified the anomaly in Region I as the core of a large subhorizontal remnant of slab (Figure 3b). Evidently, this remnant also has a strong petrofabric.

[17] LPO of α-phase is commonly accepted as the cause of strong anisotropy in the lithosphere [e.g., *Savage*, 1999], so in general such an interpretation seems feasible for anisotropy in subducted slab. In contrast, SPO of hydrous phases or melt pockets requires a regional stress pattern and therefore seems inconsistent with the lack of clear patterns in the fault plane solutions of OE [*CB2001*]. This observation also implies that LPO of α-phase is probably a preserved fossil fabric, not formed by active flow that also requires a regional stress pattern.

[18] Additional considerations also favor metastable olivine to explain reduction of V in Region I. If partial melt is the primary cause, the amount of reduction in V_S should be

much greater than that in V_P, inconsistent with comparable values of 2–3% observed for both [*BC2003*]. To reduce V by 2–3% under subsolidus conditions calls for too much low-density hydrous phases, making the slab buoyant throughout the mantle and unable to subduct [*BC2000*].

[19] For metastable olivine to work, about 60% of olivine-polymorph should remain in α-phase [*BC2000*; *BC2003*]. This estimate brings out a subtle, but intriguing point. As a cold slab descends into the TZ and leaves the stability field of α-phase, metastable olivine would make the leading edge of slab buoyant [e.g., *Bina*, 1996; *Marton et al.*, 1999]. However, this portion will never float above the 410-km discontinuity where warmer olivine of the ambient mantle is also in α-phase. So buoyancy of the slab is a self-limiting process confined to the TZ [*BC2000*; *BC2003*; *CB2001*]. This process offers a natural explanation for the subhorizontal configuration of slab remnant that appears to be detached from actively subducting lithosphere (Figure 3b). Moreover, a buoyant slab favors retention of subducted material in the TZ and hinders slab penetration into the lower mantle, a key issue pertaining to the current debate of mantle convection and mixing [e.g., *CB2001*].

[20] The remaining issues are the exact origin of the slab remnant and associated anisotropy. It is exceedingly difficult to unravel the detailed history of a detached slab, as it would leave little trace in the geologic record near the surface. Under limited azimuthal coverage and geometry of ray-paths, one must assume that the approximately north-south polarization of *SH* is close to the true fast polarization direction (Figure 1a). For dry olivine, the alignment of *a*-axes or flow direction would be approximately north-south. Since fossil fabric in the oceanic lithosphere is believed to form during seafloor spreading and align normal to the ridge axis [e.g., *Savage*, 1999], a north-south trending fabric is consistent with detached lithosphere from past convergence along the fossil Vitiaz trench where subduction ceased about 5–8 Ma ago (Figure 3b) [*Hamburger and Isacks*, 1987; *Okal and Kirby*, 1998]. However, the relationship between LPO and direction of flow may depend on water content and stress level, thus being non-unique [e.g., *Jung and Karato*, 2001]. So one cannot rule out an alternative hypothesis that due to its buoyancy, the detached slab may have broken off from actively subducting slab [*Green*, 2001].

[21] In any case, contrary to conventional notions, fast subduction of cold slab seems to favor a petrologic anomaly that is buoyant and stagnates in the TZ. At this stage, the petrologic anomaly masks the effect of low temperature to raise V. Instead, the core of slab manifests itself through seismic anisotropy and seismicity in the TZ (Region I). In the cold aureole that is expected to surround this petrologic anomaly (Region II), or in a thermal anomaly that has been partially assimilated, the petrologic anomaly has dissipated by phase transformation or dehydration, so anisotropy and seismicity cease but high V is still expected as low temperature remains to affect such measurements. Any remaining thermal anomaly is gradually assimilated (Region III), eventually being indistinguishable from the background.

[22] **Acknowledgments.** E. Matzel and R. Nowack assisted with computations. Two anonymous reviews helped improve the manuscript. This work was supported by NSF Grant 98-04718.

References

Backus, G. E., Long-wave elastic anisotropy produced by horizontal layering, *J. Geophys. Res.*, *67*, 4427–4440, 1962.

Bevis, M., F. W. Taylor, B. E. Schutz, J. Recy, B. L. Isacks, S. Helu, R. Singh, E. Kendrick, J. Stowell, B. Taylor, and S. Calmant, Geodetic observations of very rapid convergence and back-arc extension at the Tonga arc, *Nature*, *374*, 249–251, 1995.

Bina, C. R., Phase transition buoyancy contributions to stresses in subducting lithosphere, *Geophys. Res. Lett.*, *23*, 3563–3566, 1996.

Brudzinski, M. R., and W.-P. Chen, Variations of *P* wave speeds and outboard earthquakes: Evidence for a petrologic anomaly in the mantle transition zone, *J. Geophys. Res.*, *105*, 21,661–21,682, 2000.

Brudzinski, M. R., and W.-P. Chen, A petrologic anomaly accompanying outboard earthquakes beneath Fiji-Tonga: Corresponding evidence from broadband P and S waveforms, *J. Geophys. Res.*, in press, 2003.

Chen, W.-P., and M. R. Brudzinski, Evidence for a large-scale remnant of subducted lithosphere beneath Fiji, *Science*, *292*, 2475–2479, 2001.

Faul, U. H., D. R. Toomey, and H. S. Waff, Intergranular basaltic melt is distributed in thin, elongated inclusions, *Geophys. Res. Lett.*, *21*, 29–32, 1994.

Fuchs, K., and G. Mueller, Computation of synthetic seismograms with the reflectivity method and comparison with observations, *Geophys. J. R. Astron. Soc.*, *23*, 417–433, 1971.

Gajewski, D., and I. Psencik, Computation of high-frequency seismic wavefield in 3-D laterally varying layered anisotropic structures, *Geophys. J. R. Astron. Soc.*, *91*, 383–411, 1987.

Green, H. W., and P. C. Burnley, A new self-organizing mechanism for deep-focus earthquakes, *Nature*, *341*, 733–737, 1989.

Green, H. W., II, A graveyard for buoyant slabs?, *Science*, *292*, 2445–2446, 2001.

Hamburger, M. W., and B. L. Isacks, Deep earthquakes in the southwest Pacific: A tectonic interpretation, *J. Geophys. Res.*, *92*, 13,841–13,854, 1987.

Isacks, B., and P. Molnar, Distribution of stresses in the descending lithosphere from a global survey of focal-mechanism solutions of mantle earthquakes, *Rev. Geophys.*, *9*, 103–174, 1971.

Jung, H., and S.-I. Karato, Water-induced fabric transitions in olivine, *Science*, *293*, 1460–1462, 2001.

Karato, S.-I., Seismic anisotropy in the deep mantle, boundary layers and the geometry of mantle convection, *Pure Appl. Geophys.*, *151*, 565–587, 1998.

Kirby, S. H., W. B. Durham, and L. A. Stern, Mantle phase changes and deep-earthquake faulting in subducting lithosphere, *Science*, *252*, 216–225, 1991.

Lay, T., The fate of descending slabs, *Annu. Rev. Earth Planet. Sci.*, *22*, 33–61, 1994.

Marton, F. C., C. R. Bina, S. Stein, and D. C. Rubie, Effects of slab mineralogy on subduction rates, *Geophys. Res. Lett.*, *26*, 119–122, 1999.

Meade, C., and R. Jeanloz, Deep-focus earthquakes and recycling of water into the earth's mantle, *Science*, *252*, 68–72, 1991.

Okal, E. A., and S. H. Kirby, Deep earthquakes beneath the Fiji Basin, SW Pacific: Earth's most intense deep seismicity in stagnant slabs, *Phys. Earth Planet. Inter.*, *109*, 25–63, 1998.

Savage, M. K., Seismic anisotropy and mantle deformation: what have we learned from shear wave splitting?, *Rev. Geophys.*, *37*, 65–106, 1999.

Silver, P. G., Seismic anisotropy beneath the continents: Probing the depths of geology, *Annu. Rev. Earth Planet. Sci.*, *24*, 385–432, 1996.

Silver, P. G., R. W. Carlson, and P. Olson, Deep slabs, geochemical heterogeneity and the large-scale structure of mantle convection, *Annu. Rev. Earth Planet. Sci.*, *16*, 477–541, 1988.

Trampert, J., and H. J. van Heijst, Global Azimuthal Anisotropy in the Transition Zone, *Science*, *296*, 1297–1299, 2002.

Wookey, J., J. M. Kendall, and G. Barruol, Mid-mantle deformation inferred from seismic anisotropy, *Nature*, *415*, 777–780, 2002.

W.-P. Chen, Department of Geology, University of Illinois at Urbana-Champaign, USA. (w-chen@uiuc.edu)

M. R. Brudzinski, Department of Geology and Geophysics, University of Wisconsin at Madison, USA. (brudzins@geology.wisc.edu)